Tuning of quadratic nonlinear optical activity of chromophores with indolizine donor moiety and polyene π-bridge on the basis of electrochemical data

Yulia H. Budnikova [*], Yulia B. Dudkina, Alexey A. Kalinin, Guzel M. Fazleeva, Liliya N. Islamova, Alina I. Levitskaya, Olga D. Fominykh, Marina Yu. Balakina

A.E. Arbuzov Institute of Organic and Physical Chemistry, Kazan Scientific Centre, Russian Academy of Sciences, Arbuzov Str. 8, Kazan 420088, Russia

ARTICLE INFO

ABSTRACT

Electrochemical data (CV peak potentials, DPV potentials, frontier orbitals energy values and energy gap ΔE^{el}) were used to characterize chromophores with isomeric indolizine donor moieties, different acceptors and polyene π-bridges of various length. A good correlation was found between the electrochemical ΔE^{el}, optical ΔE^{opt} and calculated ΔE^{qch} (DFT) characteristics. Electrochemical data make it possible to determine the energies of frontier molecular orbitals independently, in contrast to ΔE^{opt} one, calculated from λ_{max} (UV-vis spectra). This advantage allows us to understand the origin of the chromophore energy gap changes when the nature of the donor, acceptor, or bridge varies. The polyene π-bridges are shown to provide better charge transfer ability compared to the hetarene-containing bridges; they are responsible for chromophore energy characteristics variation with changes in building blocks. The effect of the bridge length and the donor/acceptor end fragments is discussed. Indolizine donors produce NLO-chromophores with high first hyperpolarizability, β. The smallest $\Delta E^{el} = 0.91$ eV and the highest first hyperpolarizability - $1007 \cdot 10^{-30}$ esu are achieved for a chromophore with 1-methyl-2-(4-methoxyphenyl)indolizin-3-yl donor, 3-cyano-2-dicyanomethylene-5,5-dimethyl-2,5-dihydrofuran-4-yl acceptor and octatetraene π-bridge. The correlation between β and $1/(\Delta E^{el})^2$ is nearly linear. Polyene π-bridges provide high sensitivity of redox potentials to the nature of the donor and acceptor compared to chromophores with hetarene-containing bridges.

1. Introduction

Organic conjugated push-pull chromophores with the electron-donor (D) and electron-acceptor (A) structural blocks coupled through a conjugated π-electron bridge are widely used to develop electro-optical materials [1–4]. The use of heterocyclic systems with strong electron donating and electron-withdrawing properties as terminal fragments made it possible to noticeably improve the properties of nonlinear optical (NLO) chromophores [5–9]. The π-bridge provides conjugation between these D and A end groups, the actual electron transfer depending strongly on the nature of the bridge which is either polyene or heterocycle-containing one. As it turned out, bridges with heterocyclic cores do not always support an efficient interaction between the terminal donor and acceptor fragments, though provide achieving low values of the energy gap and the corresponding high hyperpolarizability [10]. Here we clarify the role of the polyene bridge in direct electronic

interaction between the donor and acceptor terminal fragments by the example of chromophores with isomeric indolizine donors.

Indolizine fragments are basic structural motifs in many biologically active molecules, natural and synthetic ones [11–15], they are used as organic fluorescent molecules for biological and material applications [16–18], as elements in the structure of redox-active macrocycles for redox-switching of metal cations coupling [19–23], as blocks of conjugated donor–acceptor polymers, which exhibit ambipolar semiconducting behavior [24], etc. Many practical applications of indolizine derivatives are associated with remarkable properties of near-infrared absorption [25–27] and emission with increased Stokes shifts [16–18, 28–31]. A significant π-charge on the first and third carbon atoms is a distinctive feature of indolizine moiety [32]. So far, indolizines have been studied much less than other donor blocks in NLO chromophores, although the first results on these chromophores showed certain advantages of indolizine derivatives providing high thermal stability and
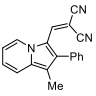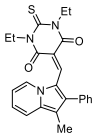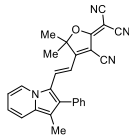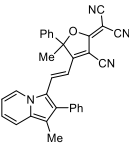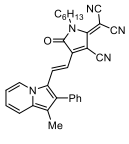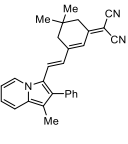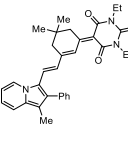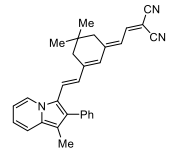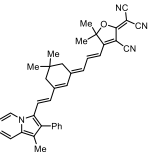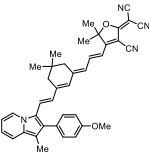
Table 1

Electrochemical (CV and DPV), optical and DFT calculated data for indolizine chromophores. Electrochemical data in CH_2Cl_2 / 0.2 M Bu_4NBF_4, substrate concentration 1–2 mM. Pt working electrode, scan rate 100 mV/s, ref. vs Fc^+/Fc, E_p^f and E_p^r are forward and return peak potentials, $E_{HOMO/LUMO} = -(E_{DPV}^{ox/red} + 4.8)$; $\Delta E = E^{LUMO}-E^{HOMO}$. ΔE^{opt} on the base of λ_{max} in CH_2Cl_2.

	A(0)W	A(0)X	A(1)Y	A(1)Y′	A(1)Z	A(2)W	A(2)X	A(3)W	A(4)Y	A′(4)Y
E_{DPV}^{ox}, V	0.72	0.63	0.51	0.54	0.48	0.12	0.08	0.03	−0.05	−0.04
E_{DPV}^{red}, V	−1.72	−1.50	−1.21	−1.21	−0.81	−1.47	−1.20	−1.32	−0.96	−0.95
Oxidation, E_p^f/ E_p^r	0.76/0.69 quasirev	0.67 irrev.	0.54/0.47 rev.	0.59/0.50 rev.	0.52 irrev.	0.16 irrev.	0.12 irrev.	0.06/−0.03 quasirev.	−0.01 irrev.	−0.01/−0.11 quasirev
Reduction, E_p^f/ E_p^r	−1.80 irrev	−1.59/ −1.50 quasirev	−1.30 irrev.	−1.29 irrev.	−0.89/−0.81 rev.	−1.56 irrev.	−1.29 irrev.	−1.41	−1.04 irrev.	−1.04 irrev.
E_{HOMO}^{el}, eV	−5.52	−5.43	−5.31	−5.34	−5.28	−4.92	−4.88	−4.83	−4.75	−4.76
E_{LUMO}^{el}, eV	−3.08	−3.30	−3.59	−3.59	−3.99	−3.33	−3.60	−3.48	−3.84	−3.85
ΔE^{el}, eV	2.44	2.13	1.72	1.75	1.29	1.59	1.28	1.35	0.91	0.91
E_{HOMO}^{qch}, eV[a]	−5.63	−5.47	−5.34	−5.49	−5.46	−5.08	−5.02	−4.96	−5.05	−5.33
E_{LUMO}^{qch}, eV[a]	−2.38	−2.51	−2.97	−2.92	−3.36	−2.57	−2.66	−2.67	−3.13	−3.44
ΔE^{qch}, eV[a]	3.24	2.96	2.37	2.57	2.10	2.51	2.35	2.30	1.92	1.89
μ, D[b]	8.4	6.6	16.9	17.4	13.3	11.8	9.5	12.9	22.8	22.8
β_{tot}, 10^{-30} esu[b]	16	21	95	83	194	176	263	373	999	1007
ΔE^{opt}, eV	2.59	2.36	1.95	1.94	1.62	2.15	1.82	2.00	1.59	1.57
Ref. [el/qch/opt]	This work	[33/33/33]	[This work /39/39]	[34/34/34]	[34/34/34]	[33/33/33]	[33/33/33]	This work	[35/32/35]	[This work/38/38]

[a] Calculated by DFT at B3LYP/6–31G(d) level.
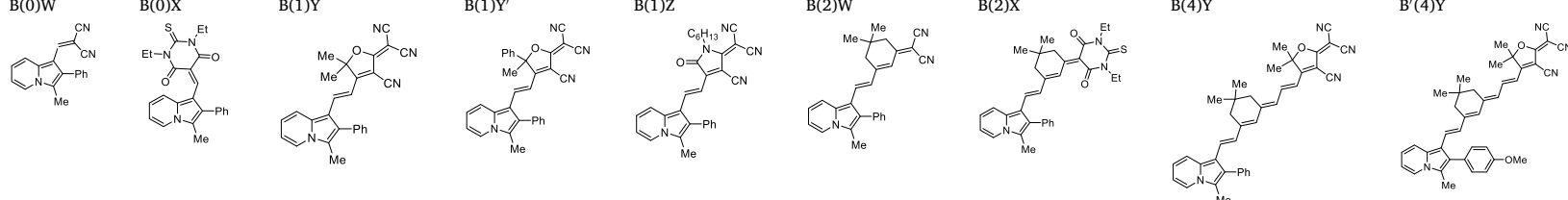[b] Calculated by DFT at M06–2X/aug-cc-pVDZ level (GAUSSIAN16).

Table 2

Electrochemical (CV and DPV), optical and DFT calculated data for indolizine chromophores. Electrochemical data in CH_2Cl_2 / 0.2 M Bu_4NBF_4, substrate concentration 1–2 mM. Pt working electrode, scan rate 100 mV/s, ref. vs Fc^+/Fc, E_p^f and E_p^r are forward and return peak potentials, $E^{HOMO/LUMO} = -(E_{DPV}^{ox/red} + 4.8)$; $\Delta E = E^{LUMO} - E^{HOMO}$. ΔE^{opt} on the base of λ_{max} in CH_2Cl_2.

	B(0)W	B(0)X	B(1)Y	B(1)Y′	B(1)Z	B(2)W	B(2)X	B(4)Y	B′(4)Y
E_{DPV}^{ox}, V	0.74	0.58	0.52	0.57	0.48	0.17	0.13	−0.02	−0.02
E_{DPV}^{red}, V	−1.89	−1.60	−1.31	−1.30	−0.84	−1.57	−1.27	−0.99	−0.99
Oxidation, E_p^f/E_p^r	0.78/ 0.70 quasirev	0.62 irrev.	0.55/0.48 rev.	0.59/0.50 rev.	0.52 irrev.	0.21 irrev.	0.17 irrev.	0.02 irrev.	0.01/−0.09 quasirev
Reduction, E_p^f/E_p^r	−1.97 irrev.	−1.68/−1.60 rev.	−1.40 irrev	−1.39 irrev.	−0.93/−0.84 rev.	−1.65 irrev.	−1.35 irrev.	−1.07 irrev.	−1.07 irrev
E_{HOMO}^{el}, eV	−5.54	−5.38	−5.32	−5.37	−5.28	−4.97	−4.93	−4.78	−4.78
E_{LUMO}^{el}, eV	−2.91	−3.20	−3.49	−3.50	−3.96	−3.23	−3.53	−3.81	−3.81
ΔE^{el}, eV	2.63	2.18	1.83	1.87	1.32	1.74	1.40	0.97	0.97
E_{HOMO}^{qch}, eV[a]	−5.0	−5.46	−5.51	−5.48	−5.46	−5.09	−5.00	−5.03	−5.33
E_{LUMO}^{qch}, eV[a]	−2.6	−2.29	−2.78	−2.75	−3.26	−2.42	−2.50	−3.04	−3.35
ΔE^{qch}, eV[a]	2.43	3.17	2.73	2.73	2.20	2.67	2.50	1.99	1.98
μ, D[b]	10.0	7.9	18.2	18.5	14.2	13.2	11.3	24.2	24.3
β_{tot}, 10^{-30} esu[b]	12	25	97	88	200	158	234	923	920
ΔE^{opt}, eV	2.64	2.38	2.08	2.07	1.68	2.25	1.88	1.62	1.61
Ref. [el/qch/opt]	This work	[33/33/33]	[This work /39/39]	[34/34/34]	[34/34/34]	[33/33/33]	[33/33/33]	[35/32/35]	[This work/38/38]

[a] Calculated by DFT at B3LYP/6–31G(d) level.

[b] Calculated by DFT at M06–2X/aug-cc-pVDZ level (GAUSSIAN16).

the advanced first hyperpolarizability [32–35]. In the previous works we have studied structure-property relationship for chromophores with dialkylarylamino donors and π-electron bridges of various nature and length which include various heterocyclic cores (quinoxaline, quinoxalinone, thiophene ones), and established the effect of the composition of the building blocks on the characteristics of the chromophores both electrochemical and molecular NLO ones [10,36,37]. In this work, we analyze the relationship between the electrochemical data and molecular NLO characteristics of a number of chromophores with isomeric indolizine donor moieties, various acceptors (cyano-containing and barbituric ones) and polyene π-bridges of different length.

2. Experimental section

2.1. Materials and instrumentation

The IR, NMR, UV–vis and ESI spectra were registered on the equipment of Assigned Spectral-Analytical Center of FRC Kazan Scientific Center of RAS. Infrared (IR) spectra were recorded on the Bruker Vector-22 FT-IR spectrometer. NMR experiments were performed with Bruker AVANCE- 400 (400 MHz for ^{1}H NMR, 100 MHz for ^{13}C NMR) spectrometer. Chemical shifts (δ in ppm) are referenced to the solvent CDCl$_3$. The ESI MS measurements were performed using an AmazonX ion trap mass spectrometer (Bruker Daltonic GmbH, Germany) in positive mode in the mass range of 200–2800. UV–vis spectra were recorded at room temperature on a UV-6100 Ultraviolet/Visible Spectrophotometer using 10 mm quartz cells. Spectra were registered with a scan speed of 480 nm/min using a spectral width of 1 nm. All samples were prepared as solutions in dichloromethane, chloroform, acetonitrile and dioxane with the concentrations ~ 2.8–3.3·10^{-5} mol L^{-1}. The melting points, mp, of chromophores were determined by Melting Point Meter MF-MP-4. Organic solvents used were purified and dried according to standard methods. The reaction progress and the purity of the obtained compounds were controlled by TLC on Sorbfil UV-254 plates with visualization under UV light. The static electric properties of the studied chromophores are calculated by the DFT in gas at the M06–2X/aug-cc-pVDZ level with chromophore geometry fully optimized at the B3LYP/6-31G(d) level.

2.2. Electrochemical investigation

Redox properties of chromophores and their precursors were studied under similar conditions in CH$_2$Cl$_2$/0.2 M Bu$_4$NBF$_4$ at Pt working electrode with scan rate 100 mV/s, the potentials were referred vs Fc$^+$/Fc. The working potential range was within +1.35 V to −2.7 V. Energy of frontier orbitals E_{HOMO} and E_{LUMO} were estimated from electrochemical data of oxidation and reduction potentials, respectively.

2.3. General procedure for synthesis of compounds A(0)W, B(0)W and A (3)W

To the stirred mixture of aldehyde-precursors (Schemes S1-S3) and malononitrile in pyridine, 3 drops of acetic acid were added and the reaction mixture was heated for 8 h at 50 C. The solvent was evaporated on a rotary evaporator, the residue was purified by column chromatography on silica gel (eluent petroleum ether – EtOAc, 20:1).

2-((1-Methyl-2-phenylindolizin-3-yl)methylene)malononitrile (A(0)W). Use of aldehyde pre- A(0)W (30 mg, 0.13 mmol), malononitrile (12.6 mg, 0.13 mmol) and pyridine (0.2 mL) in general procedure afforded the title compound A(0)W (24 mg, 67%) as orange powder. Mp 182–183 °C, R_f 0.17 (hexane/EtOAc 1:0.1). IR (KBr, ν_{max}/cm^{-1}): 2923 (CH), 2853 (CH), 2206 (CN), 1569 (C-N, C=C), 1500, 1462, 1435, 1373, 1356, 1307, 1249, 1133, 1086, 907, 827. ^{1}H NMR (400 MHz, CDCl$_3$) δ 8.44 (d, *J* = 6.9 Hz, 1H, H5 indolizine), 7.59 (d, *J* = 8.7 Hz, 1H, H8 indolizine), 7.56–7.45 (m, 3H, *m,p*-Ph), 7.42 (s, 1H, -CH=C(CN)$_2$), 7.36 (dd, *J* = 8.7, 6.7 Hz, 1H, H7 indolizine), 7.30 (d, *J* = 6.9 Hz, 2H, *o*-pH), 7.14 (dd, *J* =

6.9, 6.7 Hz, 1H, H6 indolizine), 2.27 (s, 3H, CH$_3$). ^{13}C NMR (100 MHz, CDCl$_3$) δ 141.2 (CH), 140.8 (C), 140.2 (C), 132.3 (C), 130.4 (CH), 130.2 (CH), 128.9 (CH), 128.6 (CH), 126.3 (CH), 119.6 (C), 117.8 (C), 117.3 (C), 115.3 (C), 115.2 (C), 114.4 (CH), 9.1 (CH). ESI MS for C$_{19}$H$_{14}$N$_3$ [M+H]$^+$ 284.17.

2-((3-Methyl-2-phenylindolizin-1-yl)methylene)malononitrile (B(0)W). Use of aldehyde pre- B(0)W (50 mg, 0.21 mmol), malononitrile (21 mg, 0.21 mmol) and pyridine (0.2 mL) in general procedure afforded the title compound B(0)W (45 mg, 75%) as orange powder. Mp 191–192 °C, R_f 0.2 (hexane/EtOAc 1:0.1). IR (KBr, ν_{max}/cm^{-1}): 3108 (CH), 3055 (CH), 2912 (CH), 2213 (CN), 1573 (C-N, C=C), 1557, 1484, 1446, 1403, 1375, 1349, 1313, 1256, 1155, 1094, 933, 824. ^{1}H NMR (400 MHz, CDCl$_3$) δ 8.14–8.11 (m, 1H, H8 indolizine), 8.01 (d, *J* = 6.9 Hz, 1H, H5 indolizine), 7.59 (s, 1H, -CH=C(CN)$_2$), 7.53–7.41 (m, 4H, *m,p*-Ph, H7 indolizine), 7.29–7.27 (m, 2H, *o*-Ph), 7.10 (dd, *J* = 6.9, 6.7 Hz, 1H, H6 indolizine), 2.45 (s, 3H, CH$_3$). ^{13}C NMR (100 MHz, CDCl$_3$) δ 151.7 (CH), 134.5 (C), 132.2 (C), 131.5 (C), 130.8 (CH), 128.8 (CH), 128.2 (CH), 124.9 (CH), 124.3 (CH), 122.8 (C), 121.1 (CH), 117.0 (C), 116.0 (C), 115.0 (CH), 108.1 (C), 10.1 (CH). ESI MS for C$_{19}$H$_{14}$N$_3$ [M+H]$^+$ 284.16.

2-((E)−2-(5,5-Dimethyl-3-((E)−2-(1-methyl-2-phenylindolizin-3-yl) vinyl)cyclohex-2-en-1-ylidene)ethylidene)malononitrile (A(3)W). Use of aldehyde pre-A(3)W (17 mg, 0.04 mmol), malononitrile (4 mg, 0.04 mmol) and pyridine (0.2 mL) in general procedure afforded the title compound A(3)W (10 mg, 53%) as dark powder. Mp 203–205 °C, R_f 0.33 (hexane/EtOAc 1:0.1). IR (KBr, ν_{max}/cm^{-1}): 2949 (CH), 2926 (CH), 2213 (CN), 1574 (C-N, C=C), 1514, 1468, 1448, 1393, 1372, 1346, 1303, 1274, 1244, 1203, 1183, 1134, 1074, 1016, 950, 884. ^{1}H NMR (400 MHz, CDCl$_3$) 8.29 (d, *J* = 6.9 Hz, 1H, H-5 indolizine), 8.26 (d, *J* = 7.0 Hz, 4H, H-5 indolizine), 7.84 (d, *J* = 12.7 Hz, 1H), 7.67 (d, *J* = 12.8 Hz, 4H), 7.55–7.39 (m, 20H, *m,p*-Ph, H-8 indolizine), 7.38–7.32 (m, 10H, *o*-Ph), 7.05 (d, *J* = 16.0 Hz, 5H, ethene), 6.90–6.85 (m, 5H, H-7 indolizine), 6.76–6.69 (m, 5H, H-6 indolizine), 6.50 (d, *J* =16.1 Hz, 1H, ethene), 6.47–6.39 (m, 9H), 6.24 (d, *J*=12.9 Hz, 1H, ethene), 6.05 (s, 4H), 2.35 (s, 8H, CH$_2$), 2.32 (s, 2H, CH$_2$), 2.30 (s, 8H, CH$_2$), 2.29 (s, 2H, CH$_2$), 2.23 (s, 3H, CH$_3$), 2.22 (s, 12H, CH$_3$), 1.01 (s, 24H, CH$_3$), 0.99 (s, 6H, CH$_3$). ^{13}C NMR (100 MHz, CDCl$_3$, * the presented signals correspond to the minor isomer) δ 157.5* (C), 157.4 (C), 154.1 (CH), 153.5* (CH), 151.3 (C), 135.7, 134.94, 134.87*, 133.5, 131.0* (CH), 130.9 (CH), 129.1 (CH), 129.0* (CH), 128.5 (CH), 128.1 (CH), 128.0* (CH), 125.2 (CH), 125.0* (CH), 124.2* (CH), 124.0 (CH), 122.0 (CH), 121.6* (CH), 121.1 (CH), 120.9* (CH), 119.7 (CH), 118.4 (CH), 116.2, 116.0*, 113.9, 112.9 (CH), 112.1, 111.7*, 40.7* (CH), 40.4 (CH), 39.7* (CH), 39.4 (CH), 32.2* (C), 31.9 (C), 28.9 (CH), 28.7* (CH), 9.5 (CH). ESI MS for C$_{30}$H$_{27}$N$_3$ [M]$^+$ 429.34.

3. Results and discussion

Indolizine heterocycle, being a π-excessive one, is shown to serve a new promising donor component in NLO chromophores [32–35,38,39]. Here we have studied various chromophores with polyene π-bridges of different length (n from 1 to 4 units), as well as the case when end D and A fragments are directly coupled with each other (*n* = 0, Tables 1 and 2). Donor fragments are isomeric 1(3)-methyl-2-phenylindolizin-3(1)-yl moieties (A and B) and their 2-methoxyphenyl analogues (A′ and B′); acceptor moieties are dicyanovinyl (W), 1,3-diethylthiobarbituric methylene (X), 3-cyano-2-dicyanomethylene-5,5-dimethyl-2,5-dihydrofuran-4-yl (Y), its 5-Ph analogue (Y′) and 4-cyano-5-dicyanomethylene-2-oxo-2,5-dihydropyrrol-3-yl (Z) ones.

New chromophores A(0)W, B(0)W and A(3)W with dicyanovinyl acceptor moieties have been synthesized via Knoevenagel condensation of corresponding aldehyde precursors and malononitrile (Schemes S1-S3). These aldehydes and other chromophores were obtained according to literature [33–35,38,39]. The elongation of π-bridge from *n* = 0 to *n* = 3 results in the bathochromic shift of absorption maximum (up to Δλ$_{max}$ 150 nm) and essential increase of positive chloroform-dioxane solvatochromic shift from 6 (0.03 eV) to 44 nm (0.15 eV) (Fig. S1,
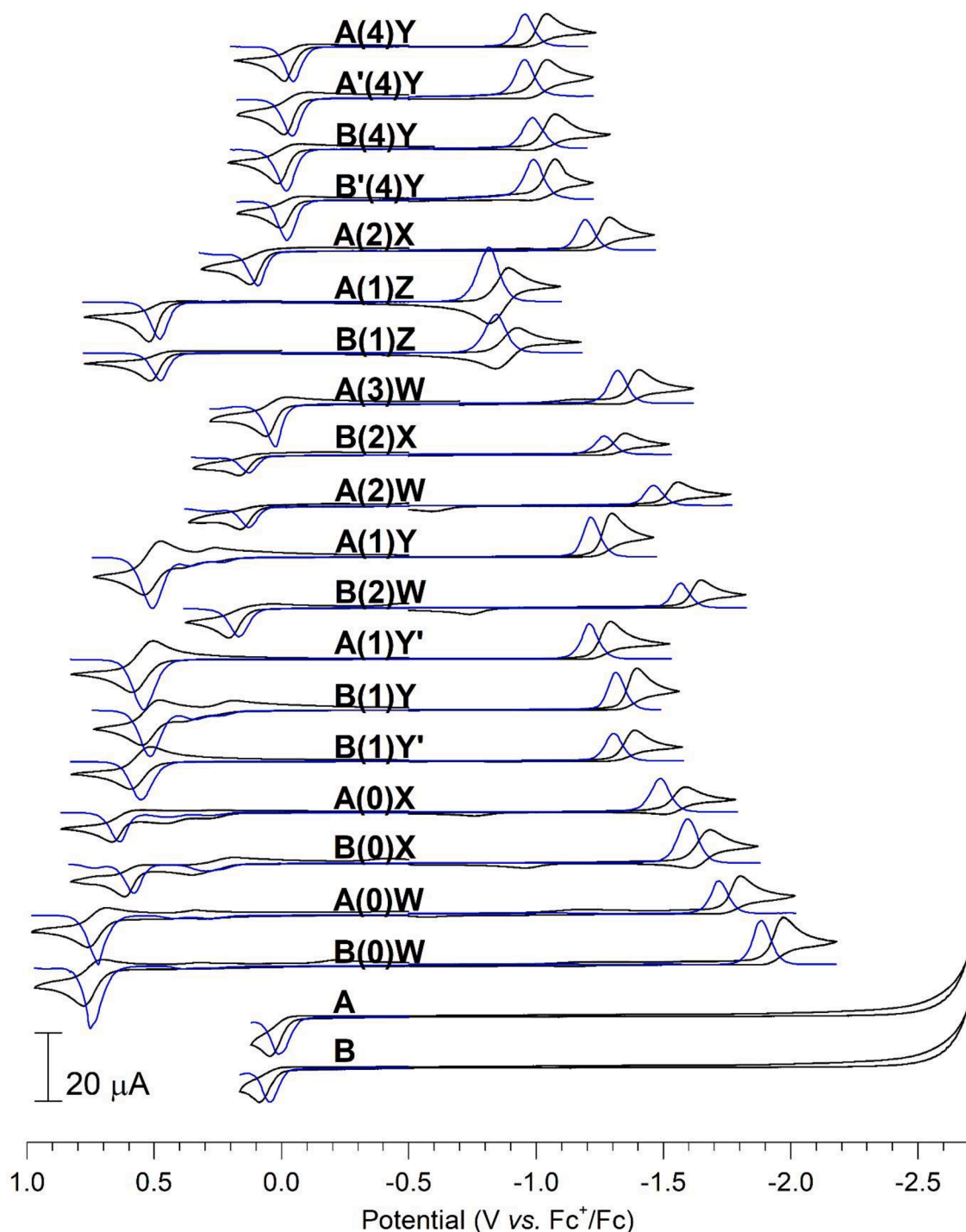
Fig. 1. CVs (black) and DPVs (blue) of chromophores building blocks illustrating electrochemical data from Tables 1, 2 and S1.

Table S1). In case of stronger acceptor, the elongation of π-bridge by three vinylene units (from $n = 1$ to $n = 4$) when passing from A(1)Y to A(4)Y leads to greater increase of solvatochromic shift from 13 (0.04 eV) to 78 nm (0.19 eV) [35,39].

The redox properties of the studied chromophores along with the DFT estimations of electric properties (dipole moments and first hyperpolarizabilities) are presented in Tables 1 and 2; the corresponding redox curves are given in Fig. 1. The electrochemical data for D/A compounds – components of the studied chromophores, are given in Table S2.

3.1. The effect of the bridge length

The effect of the bridge length on the oxidation potential is demonstrated by the example of chromophores with dicyanovinylene acceptors: A(0)W, A(2)W and A(3)W. The elongation of the bridge up to 3 vinylene units results in the decrease of the oxidation potential by ~0.7 V (app. 0.23 V per vinylene unit). However, such estimation is rather rough as the effect of elongation is attenuated with the increase of n: when passing from A(0)W to A(2)W oxidation potential decreases by 0.6 V (app. 0.3 V per vinylene unit), while passing from A(2)W to A(3)W the decrease is 0.1 V. For the case of chromophores with X acceptor the
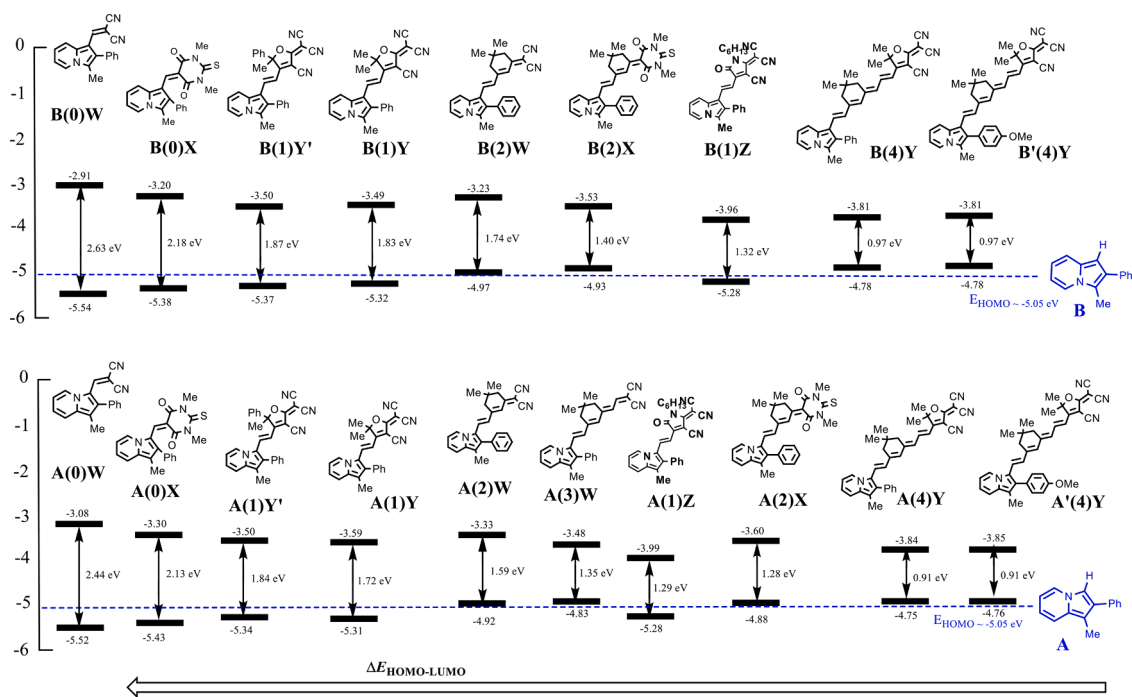
Fig. 2. Dependence of the energies of the frontier orbitals calculated electrochemically from DPVs on the structure of indolizine chromophores.

elongation of the bridge by two vinylene units (from A(0)X to A(2)X) causes the decrease of the oxidation potential by 0.55 V (app. 0.28 V per vinylene unit). When chromophores with Y acceptor are considered (A(1)Y and A(4)Y), the effect is less pronounced: E_p^{ox} ox reduces from 0.54 V to −0.01 V (app. 0.18 V per vinylene unit). Similar picture is observed for relative chromophores with isomeric B donor.

As for reduction potentials, the effect of the bridge elongation is less pronounced: the decrease of E_p^{red} is app 0.1–0.15 V per vinylene unit. Earlier it was shown [10] that when the bridge is elongated by vinyl-hetaryl unit, the decrease of E^{red} is 0.25–0.50 V depending on the nature of the hetaryl core (thiophene<quinoxaline<quinoxalinone).

As the values of redox potentials correlate with LUMO/HOMO energies, the effect of bridge elongation on E_{LUMO} and E_{HOMO} reflects the observed tendencies (Fig. 1): at bridge elongation by three vinylene units the destabilization of HOMO is greater than the stabilization of LUMO (0.53–0.69 eV and 0.25–0.4 V, correspondingly). These effects result in the notable decrease of ΔE^{el} by 0.82–0.89 V when n changes from 0 to 2; the increase of the bridge from 1 to 4 produces similar changes in ΔE^{el}, while the change of n from 0 to 3 provides greater change of ΔE^{el} − 1.09 V. This indicates that the effect attenuates with the addition of each subsequent unit, i.e., there is no need for a significant lengthening of the bridge.

Similar tendency in the change of energy gap is observed when ΔE is estimated both quantum-chemically, ΔE^{qch}, and on the basis of UV–Vis experiment, ΔE^{opt}: the elongation of the bridge results in the decrease of the energy gap value. As according to the two-state model (TSM) [40], the first hyperpolarizability depends on the difference between the excited and ground state dipole moments, (μ_{ee}-μ_{gg}), the transition dipole moment μ_{ge}, and the transition energy ΔE_{ge}:

$$\beta \propto \frac{(\mu_{ee} - \mu_{gg})\mu_{ge}^2}{\Delta E_{ge}^2},$$

one may note, that ΔE^{qch} can serve as a marker providing useful guidelines for selection of effective NLO chromophores.

The changes in ΔE^{el} are accompanied by the essential growth of β_{tot}; when the bridge length increases from 0 to 2, β_{tot} becomes 10 times higher: in the case of X acceptor ΔE^{el} changes from 2.13 eV to 1.28 eV,

what correlates with the growth of β_{tot} from 21 10−30 to 263 10−30 esu; for W acceptor ΔE^{el} changes from 2.44 eV to 1.59 eV and β_{tot} grows from 16 10−30 to 176 10−30 esu. One may note that the effect of bridge elongation from $n = 0$ to $n = 2$ is comparable with that for the case when n changes from 1 to 4: for chromophores with Y acceptor the value of β_{tot} increases from 95 10−30 to 999 10−30 esu.

3.2. The effect of the end D/A fragments

According to the redox characteristics of the chromophore's donor groups, one may conclude that indolizine A fragment possesses higher electron donating ability than the B one: the oxidation potential of A is somewhat smaller. Thus the ΔE^{el} of chromophores with A donor moiety is in all cases lower than for chromophores with B donor, and, correspondingly, the value of β_{tot} is higher (Tables 1, 2). As for the acceptor components, they may be ranged in accordance with the values of reduction potential and corresponding electron withdrawing ability as follows: W, X, Y and Z.

The effect of the acceptor on the reduction potential and ΔE^{el} is manifested at fixed length of the bridge in accordance with the E^{red} of the compounds-acceptors W, X, Y and Z (Tables 1, 2). For these compounds, the lower E^{red}, the greater acceptor strength; thus the acceptor, being a component of a chromophore, affects stronger chromophore characteristics, in particular, the value of E_p^{red}; the effect on E_p^{ox} is inessential. For the case $n = 0$ E_p^{red} A(0)X/B(0)X is equal to −1.59/−1.68 V, what is notably smaller than for A(0)W/B(0)W − −1.80/−1.97 V; similar tendency holds for $n = 2$: E_p^{red} for A(2)X/B(2)X is equal to −1.29/−1.35 V, what is notably smaller than for A(2)W/B(2)W − −1.56/−1.65 V. This is in accordance with E_p^{red} for the compound-acceptors (Table S1): for X E_p^{red} is −1.82 V and for W − 2.07 V.

The electron-withdrawing strength of Z acceptor is higher than that of Y [9] (compound Y), this fact manifests itself at the comparison of E_p^{red} for chromophores A(1)Z/B(1)Z and A(1)Y/B(1)Y with $n = 1$: E_p^{red} is equal to −0.89/−0.93 V and −1.30/−1.40 V, respectively. One may note that the presence of other substituent in the acceptor fragment (Ph instead of Me in A(1)Y'/B(1)Y') as well as in the donor fragment (MeOC$_6$H$_4$ instead of Ph in A'(4)Y/B'(4)Y) almost does not affect the values of E_p^{red}. Similar tendencies are observed for ΔE^{el} values; the
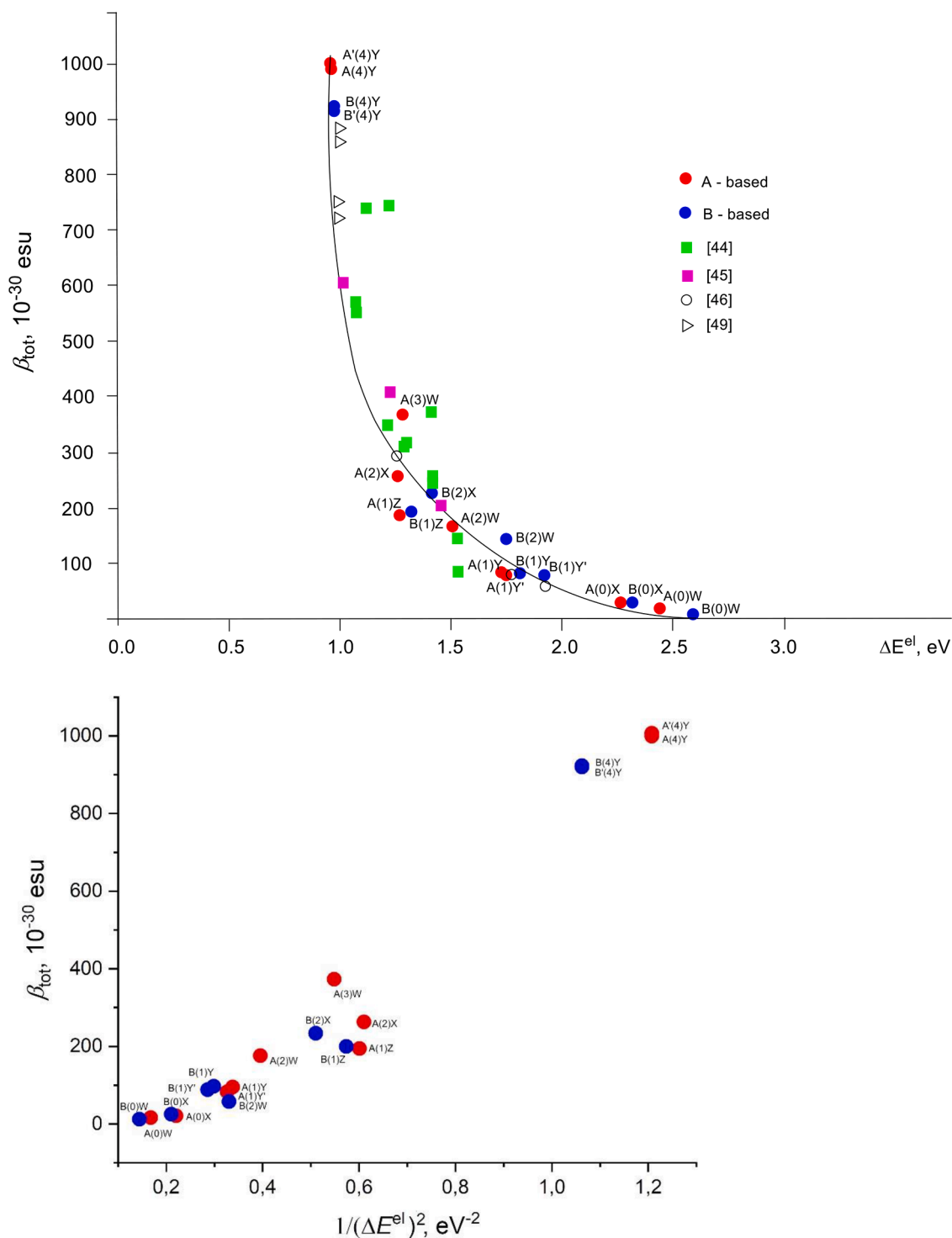
Fig. 3. The dependencies β_{tot} on ΔE^{el} for the studied chromophores and for chromophores previously described [44-46,49] (top) and β_{tot} on $1/(\Delta E^{el})^2$ (bottom) for the studied chromophores (red points for A-based indolizines, blue ones for B-based indolizines).

introduction of stronger acceptor fragment causes the decrease of ΔE^{el} and the increase of β_{tot} values: for A(1)Y/B(1)Y and A(1)Z/B(1)Z ΔE^{el} is equal to 1.72/1.83 eV and 1.29/1.32 eV, the values of β_{tot} being 95 10^{-30}/97·10^{-30} esu and 194 10^{-30}/200·10^{-30} esu, respectively. This tendency also holds for ΔE^{qch} and ΔE^{opt}. One may note, that the change of the acceptor results in the essential change of the reduction potential (see, for example, the data for A(1)Y and A(1)Z, A(2)W and A(2)X); however, it results in the smaller change of oxidation potential. As it was shown earlier, similar trends are observed for chromophores with

quinoxaline moiety in the π-bridge [10], as well as for literature chromophores with octatetraene bridge [5] (Fig. 2).

Keeping in mind the inverse dependence of β on ΔE^2_{ge}, determined by TSM, we have considered the correlation between β and ΔE^{el}, which is also shown to hold for chromophores of different nature, varying by donors, acceptors, and π-bridges (Figs. 3, S8). The plot of β vs ΔE^{el} is approximated by an inverse quadratic function, the plot of β vs $(\Delta E^{el})^{-2}$ is nearly linear (Fig. 3).

To demonstrate that the easily available electrochemical gap can be

Table 3
Composition analysis for HOMO and LUMO of the A-type chromophores; contribution (in%) from the fragments – donor (D), π-bridge (B), acceptor (A).

	D	A(0)W			A(1)W			A(2)W			A(3)W	A(0)X		A(2)X			A(1)Y			A(4)Y		
		A	D	B	A	D	B	A	D	B	A	D	A	D	B	A	D	B	A	D	B	A
HOMO	71.5	28.5	57.0	17.0	26.0	53.7	29.0	17.3	47.3	37.7	15.0	53.4	46.6	52.2	30.1	17.8	47.2	14.6	38.3	40.6	42.5	16.9
LUMO	42.3	57.7	34.1	24.0	41.9	22.5	42.2	35.3	16.5	49.6	33.9	44.6	55.4	19.4	52.7	27.9	31.0	21.7	47.3	12.3	53.1	34.6

helpful for the choice of effective NLO chromophores, we have attracted literature data for various types of compounds including chromophores both with polyene and hetarene-containing bridges (Tables S3–S7). An analysis of the literature data on electrochemical gaps and calculated hyperpolarizabilities of various chromophores shows that in most cases the smaller the gap, the greater the hyperpolarizability. Interestingly, for the β vs. ΔE^{el} plot the points corresponding to the data for chromophores of different nature, both studied in this work and literature ones, lie on the same curve (Fig. 3). Tables S3–S5 show the impact of chromophore donor [41–43], π-electron bridge [10,44–46] and acceptor moieties [45, 47–49] on the first hyperpolarizabilities and electrochemical gaps, respectively. We found three types of deviations from this regularity: first, introduction of bulky groups containing heteroatoms or aryl fragments into the bridge results in breaking the tendency, however in this case the gap changes are very small (Table S6) [47,50]. Second, the electrochemically determined gap becomes drastically small, while first hyperpolarizability does not become outstandingly high, this case is a unique one (Table S3, series 3) [42]. Third violation is typical for isomeric chromophores, varying by the site of attachment of donor-vinylene moiety to the bridge hetarene moiety (Table S7) [48, 51].

3.3. Composition analysis for frontier orbitals

As HOMO and LUMO energies play a crucial role in our discussion, it is useful to consider how different structural components of the chromophores contribute into the frontier orbitals (Fig. S9). We have performed HOMO and LUMO composition analysis in the framework of MULTIWFN program (estimation of contributions by Hirshfeld method) [51]; the results of the analysis are presented in Tables 3, 4 for A and B donor-based chromophores with different acceptors and varying bridge length.

According to the obtained data, HOMO is delocalized over indolizine donor (both for chromophores of A- and B-type, Tables 3 and 4, respectively) and polyene bridge, the percentage of the bridge contribution depending on the bridge length. The largest bridge contribution was obtained for A(4)W with octatetraene bridge. In the case when D and A are directly coupled, the contribution from D decreases with the increase of the acceptor strength, while contribution from acceptor increases (Table 3). This observation is less pronounced for chromophores with $n = 1$ and becomes inessential for longer bridges (Fig. S10).

As for LUMO composition, it has high contribution not only from the acceptor but also from the bridge for all the chromophores studied here. Similar situation was described for molecules with triazene moiety in the bridge [52], as well as for D-π-A chromophores with polyene and thiophene-containing bridges [46,48,53–55].

The results of the analysis for B-based chromophores presented in Table 4 demonstrate similar tendencies in the changes of components contributions depending on the chromophore composition.

We have considered frontier orbitals composition for chromophores with octatetraene bridge ($n = 4$) and various acceptors (Fig. 4); A4 is a model compound composed from donor and octatetraene bridge (without an acceptor). HOMO is mainly delocalized over indolizine donor and the bridge, these contributions decreasing with the increase of the acceptor strength. Interestingly, the contribution from the acceptor, being comparatively small, nevertheless increases with the acceptor strength. As for LUMO, it embraces the bridge and the acceptor, the latter contribution increasing with the acceptor strength.

4. Conclusion

In the present paper redox and NLO characteristics of two series of chromophores with isomeric indolizine A and B donors, polyene bridges of different length and electron acceptors of varying strength are analyzed. The effect of chromophores structural components on the values of E^{ox}, E^{red} and ΔE^{el} as well as on first hyperpolarizability values

Table 4

Composition analysis for HOMO and LUMO of the B-type chromophores; contribution (in%) from the fragments – donor (D), π-bridge (B), acceptor (A).

	B(0)W		B(2)W			B(1)Y			B(4)Y		
	D	A	D	B	A	D	B	A	D	B	A
HOMO	71.06	28.94	50.63	30.98	18.38	45.32	14.85	39.83	34.91	46.20	18.89
LUMO	47.11	52.89	19.71	42.98	37.31	27.71	21.79	50.51	10.00	53.74	36.27
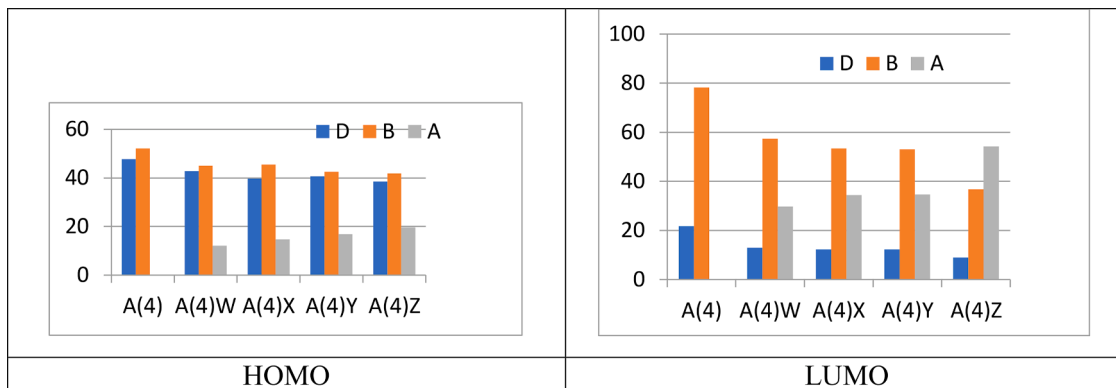
Fig. 4. Contributions into frontier orbitals for chromophores with octatetraene bridge and different acceptors from various fragments (in%).

is specially considered. E^{ox} potential of A is found to be lower than that of B; when A and B moieties are incorporated in the chromophores, the values of E^{ox} and E^{red} for chromophores with A donors are as a rule lower than those for B-based chromophores, thus producing smaller ΔE^{el} and higher β_{tot} values for A-based chromophores in all cases. Similarly, at a given length of polyene bridge the introduction into the chromophore the compound-acceptors W-Z, characterized by E^{red} decreasing from W to Z, causes the decrease of E^{ox}, E^{red} and ΔE^{el} and the growth of β_{tot}. It is worth stressing that the pointed effect is most pronounced at short bridge. The observed tendency in the change of studied electrochemical and NLO characteristics holds when the π-electron bridge is elongated; the A(4)Y and A′(4)Y chromophores with the longest bridge and the most strong acceptor are characterized by the smallest ΔE^{el} – 0.91 eV and the highest first hyperpolarizability values – ~$1000 \cdot 10^{-30}$ esu. Measured ΔE^{opt} and calculated ΔE^{qch} reproduce the tendencies in ΔE^{el} changes. Chromophores with indolizine donors, polyene π-bridges and various acceptor fragments provide higher sensitivity of redox potentials to the chromophore composition compared to chromophores with hetarene containing bridges [10]. The dependence of hyperpolarizability β on ΔE^{el} gap is inverse quadratic (the bigger the gap, the smaller β). The dependence of β on $(\Delta E^{el})^{-2}$ is nearly linear, and this conclusion also extends to the data for previously described literature chromophores of different nature. Thus, the experimentally determined ΔE^{el} can provide additional evidence for NLO chromophores effectiveness.

Credit author statement

Y. Budnikova: Writing - Original Draft, Data Curation, Conceptualization, Methodology, Validation, Supervision. M. Balakina: Formal analysis, Writing - Review & Editing. Y. Dudkina: Investigation, Validation. A. Kalinin: Methodology, Validation, Writing - Review & Editing. G. Fazleeva and L. Islamova: Synthesis of chromophores, characterization; A. Levitskaya: DFT calculations; O. Fominykh: DFT calculations.

Declaration of Competing Interest

The authors declare that they have no known competing financial interests or personal relationships that could have appeared to influence the work reported in this paper.

Authors declare no known competing interests relating to research, financial benefit, authorship and/or publication.

Data Availability

Data will be made available on request.

Supplementary materials

Supplementary material associated with this article can be found, in the online version, at doi:10.1016/j.electacta.2023.142547.

References

[1] P. Guenter, Nonlinear Optical Effects and Materials, Springer, Berlin, 2002.
[2] J. Liu, C. Ouyang, F. Huo, W. He, A. Cao, Progress in the enhancement of electro-optic coefficients and orientation stability for organic second-order nonlinear optical materials, Dyes Pigment. 181 (2020), 108509, https://doi.org/10.1016/j.dyepig.2020.108509.
[3] M. Yang, M. Peng, Z. Li, Z. Wang, F. Liu, W. Liu, J. Liao, T. Luo, J. Wang, Design and synthesis of Phenylaminothiophene donor-based chromophore with enhanced electro-optic activity, Dyes Pigment. 192 (2021), 109423, https://doi.org/10.1016/j.dyepig.2021.109423.
[4] R. Bano, M. Asghar, T.Mahmood K.Ayub, J. Iqbal, S. Tabassum, R. Zakaria, M. A. Gilan, A theoretical perspective on strategies for modeling high performance nonlinear optical materials, Front. Mater. 8 (2021), 783239, https://doi.org/10.3389/fmats.2021.783239.
[5] XH. Zhou, J. Luo, J.A. Davies, S. Huanga, A.K.Y. Jen, Push–pull tetraene chromophores derived from dialkylaminophenyl, tetrahydroquinolinyl and julolidinyl moieties: optimization of second-order optical nonlinearity by fine-tuning the strength of electron-donating groups, J. Mater. Chem. 22 (2012) 16390–16398, https://doi.org/10.1039/c2jm32848h.
[6] S.M. Sharipova, A.A. Kalinin, 3-Cyano-2-(dicyano)methylene-4-methyl-2,5-dihydrofurans in the synthesis of nonlinear-optical chromophores, Chem. Heterocycl. Compd. 53 (2017) 36–38, https://doi.org/10.1007/s10593-017-2017-9.
[7] H. Zhang, Y. Tian, S. Bo, L. Xiao, Y. Ao, J. Zhang, M. Li, A study on regulating the conjugate position of NLO chromophores for reducing the dipole moment and

enhancing the electro-optic activities of organic materials, J. Mater. Chem. C 8 (2020) 1380–1390, https://doi.org/10.1039/c9tc05704h.

[8] G. Noirbent, C. Pigot, TT. Bui, S. Péralta, M. Nechab, D. Gigmes, F. Dumur, Synthesis, optical and electrochemical properties of a series of push-pull dyes based on the 2-(3-cyano-4,5,5-trimethylfuran-2(5H)-ylidene) malononitrile (TCF) acceptor, Dyes Pigment. 184 (2021), 108807, https://doi.org/10.1016/j.dyepig.2020.108807.

[9] SH. Jang, J. Luo, N.M. Tucker, A. Leclercq, E. Zojer, M.A. Haller, TD. Kim, JW. Kang, K. Firestone, D. Bale, D. Lao, J.B. Benedict, D. Cohen, W. Kaminsky, B. Kahr, JL. Bredas, P. Reid, L.R. Dalton, A.K.-Y. Jen, Pyrroline chromophores for electro-optics, Chem. Mater. 18 (2006) 2982–2988, https://doi.org/10.1021/cm052861i.

[10] Y.B. Dudkina, A.A. Kalinin, G.M. Fazleeva, S.M. Sharipova, L.N. Islamova, A. B. Dobrynin, D.R. Islamov, A.I. Levitskaya, M.Y. Balakina, Y.H. Budnikova, Composing NLO chromophore as a puzzle: electrochemistry-based approach to the design and effectiveness, ChemPhysChem 22 (2021) 2313–2328, https://doi.org/10.1002/cphc.202100506.

[11] IM. Moise, E. Bîcu, A. Farce, J. Dubois, A. Ghinet, Indolizine-phenothiazine hybrids as the first dual inhibitors of tubulin polymerization and farnesyltransferase with synergistic antitumor activity, Bioorg. Chem. 103 (2020), 104184, https://doi.org/10.1016/j.bioorg.2020.104184.

[12] M.T. Islam, C. Sarkar, D.M. El-Kersh, S. Jamaddar, S.J. Uddin, J.A. Shilpi, M. S. Mubarak, Natural products and their derivatives against coronavirus: a review of the non-clinical and pre-clinical data, Phytother. Res. 34 (2020) 2471–2492, https://doi.org/10.1002/ptr.6700.

[13] D. Amariucai-Mantu, V. Antoci, M.C. Sardaru, C.M. Al Matarneh, I. Mangalagiu, R. Danac, Fused pyrrolo-pyridines and pyrrolo-(iso)quinoline as anticancer agents, Phys. Sci. Rev. (2022), https://doi.org/10.1515/psr-2021-0030.

[14] A.A. Nevskaya, A.R. Miftyakhova, L.V. Anikina, T.N. Borisova, A.V. Varlamov, L. G. Voskressensky, Tetrahedron Lett. 87 (2021), 153552, https://doi.org/10.1016/j.tetlet.2021.153552.

[15] I. Baussanne, A. Botezatu, D.C. Larosa, B. Furdui, I. O.Ghinea, S.Chierici A.Thomas, R. Dinica, M. Demeunynck, Interest of novel N-alkylpyridinium-indolizine hybrids in the field of Alzheimer's disease: synthesis, characterization and evaluation of antioxidant activity, cholinesterase inhibition, and amyloid fibrillation interference, Bioorg. Chem. 116 (2021), 105390, https://doi.org/10.1016/j.bioorg.2021.105390.

[16] A. Raghuvanshi, A.K. Jha, A. Sharma, S. Umar, S. Mishra, R. Kant, A Nonarchetypal 5,6-dihydro-2H-pyrano[3,2-g]indolizine-based solution-solid dual emissive AIEgen with multicolor tunability, Chem. Eur. J. 23 (2017) 4527–4531, https://doi.org/10.1002/chem.201605844.

[17] D. Ndaleh, C. Smith, M.L. Yaddehige, A.K. Shaik, D.L. Watkins, N.I. Hammer, J. H. Delcamp, Shortwave infrared absorptive and emissive pentamethine-bridged indolizine cyanine dyes, Org. Chem. 86 (2021) 15376–15386, https://doi.org/10.1021/acs.joc.1c01908.

[18] W.E. Meador, S.A. Autry, R.N. Bessetti, J.N. Gayton, A.S. Flynt, N.I. Hammer, J. H. Delcamp, Water-soluble NIR absorbing and emitting indolizine cyanine and indolizine squaraine dyes for biological imaging, J. Org. Chem. 85 (2020) 4089–4095, https://doi.org/10.1021/acs.joc.9b03108.

[19] V.A. Mamedov, A.A. Kalinin, A.T. Gubaidullin, S.A. Katsuba, V.V. Syakaev, I. K. Rizvanov, Sh.K. Latypov, Efficient synthesis and structure peculiarity of macrocycles with bi-indolizinylquinoxalinone moieties, Tetrahedron 69 (2013) 10675–10687, https://doi.org/10.1016/j.tet.2013.09.014.

[20] V.A. Mamedov, A.A. Kalinin, V.V. Yanilkin, N.V. Nastapova, V.I. Morozov, A. A. Balandina, A.T. Gubaidullin, O.G. Isaikina, A.V. Chernova, Sh.K. Latypov, I. A. Litvinov, Synthesis, structure, and electrochemical properties of 1(2),4(2)-dioxo-2(1),3(1)-diphenyl-7,10,13-trioxa-1,4(3,1)-diquinoxalina-2(2,3), 3(3,2)-diindolizinacyclopentadecaphane, Russ. Chem. Bull. 56 (2007) 2060–2073, https://doi.org/10.1007/s11172-007-0322-7.

[21] V.V. Yanilkin, N.V. Nastapova, A.S. Stepanov, A.A. Kalinin, V.A. Mamedov, Cation binding by 2(1),3(1)-diphenyl-1(2),4(2)-dioxo-7,10,13-trioxa-1,4(3,1)-diquinoxa-lina-2(2,3),3(3,2)-diindolizinacyclopentadecaphane and its acyclic analog, Russ. Chem. Bull. 58 (2009) 89–94, https://doi.org/10.1007/s11172-009-0013-7.

[22] V.V. Yanilkin, N.V. Nastapova, V.A. Mamedov, A.A. Kalinin, V.P. Gubskaya, Redox-switchable binding of the Mg2+ stop ions by 2(1),3(1)-diphenyl-1(2),4(2)dioxo-7,10,13-trioxa-1,4(3,1)-diquinoxaline-2(2,3),3(3,2)-diindolysine-cyclopentadecaphane, Russ. J. Electrochem. 43 (2007) 770–775, https://doi.org/10.1134/S102319350707005.

[23] D. Shi, Z. Liu, J. Ma, Z. Zhao, L. Tan, G. Lin, J. Tian, X. Zhang, G. Zhang, D. Zhang, Half-fused diketopyrrolopyrrole-based conjugated donor–acceptor polymer for ambipolar field-effect transistors, Adv. Funct. Mater. 30 (2020), 1910235, https://doi.org/10.1002/adfm.201910235.

[24] T. Kreher, H. Sonnenschein, B. Costisella, M. Schneider, Switchable electron-rich biindolizine-based macrocycles: synthesis and redox properties, J. Chem. Soc., Perkin Trans. 1 (1997) 3451–3457, https://doi.org/10.1039/A702433I.

[25] J. Huckaba, A. Yella, L.E. McNamara, A.E. Steen, J.S. Murphy, C.A. Carpenter, G. D. Puneky, N.I. Hammer, M.Khaja Nazeeruddin, M. Grätzel, J.H. Delcamp, Molecular design principles for near-infrared absorbing and emitting indolizine dyes, Chem. Eur. J. 22 (2016) 15536–15542, https://doi.org/10.1002/chem.201603165.

[26] H. Cheema, A. Baumann, E.K. Loya, P. Brogdon, L.E. McNamara, C.A. Carpenter, N. I. Hammer, S. Mathew, C. Risko, J.H. Delcamp, Near-infrared-absorbing indolizine-porphyrin push−pull dye for dye-sensitized solar cells, ACS Appl. Mater. Interfaces 11 (2019) 16474–16489, https://doi.org/10.1021/acsami.8b21414.

[27] J. Watson, R. R.Rodrigues, J.H. Delcamp, Near-infrared unsymmetrical squaraine corebased sensitizers for co-sensitized high-photocurrent dye-sensitized solar cells,

Cell Rep. Phys. Sci. 3 (2022), 100701, https://doi.org/10.1016/j.xcrp.2021.100701.

[28] J. Gayton, Sh.A. Autry, W. Meador, S.R. Parkin, G.A. Hill Jr., N.I. Hammer, J. H. Delcamp, Indolizine-cyanine dyes: near infrared emissive cyanine dyes with increased stokes shifts, J. Org. Chem. 84 (2019) 687–697, https://doi.org/10.1021/acs.joc.8b02521.

[29] J.N. Gayton, Sh. Autry, R.C. Fortenberry, N.I. Hammer, J.H. Delcamp, Counter anion effect on the photophysical properties of emissive indolizine-cyanine dyes in solution and solid state, Molecules 23 (2018) 3051–3062, https://doi.org/10.3390/molecules23123051.

[30] S. Chatterjee, W.E. Meador, C. Smith, I. Chandrasiri, M.F. Zia, J. Nguyen, A. Dorris, A. Flynt, D.L. Watkins, N.I. Hammer, J.H. Delcamp, SWIR emissive RosIndolizine dyes with nanoencapsulation in water soluble dendrimers, RSC Adv. 11 (2021) 27832–27836, https://doi.org/10.1039/d1ra05479a.

[31] T. Kim, J. Kim, Color-tunable indolizine-based fluorophores and fluorescent pH sensor, Molecules 27 (2022) 12, https://doi.org/10.3390/molecules27010012.

[32] A.I. Levitskaya, A.A. Kalinin, O.D. Fominykh, I.V. Vasilyev, M.Yu. Balakina, Nonlinear optical properties of chromophores with indolizine donors: theoretical study, Comput. Theor. Chem. 1094 (2016) 17–22, https://doi.org/10.1016/j.comptc.2016.08.021.

[33] A.A. Kalinin, G.G. Yusupova, T.I. Burganov, Y.B. Dudkina, L.N. Islamova, A. I. Levitskaya, A.R. Khamatgalimov, S.A. Katsyuba, Y.H. Budnikova, M. Yu. Balakina, Isomeric indolizine-expanded π-expanded push–pull NLO-chromophores: Synthesis and comparative study, J. Mol. Struct. 1156 (2018) 74–82, https://doi.org/10.1016/j.molstruc.2017.11.077.

[34] A.A. Kalinin, G.M. Fazleeva, T.I. Burganov, L.N. Islamova, A.I. Levitskaya, Y. B. Dudkina, G.R. Shaikhutdinova, G.G. Yusupova, M.A. Smirnov, T.A. Vakhonina, N.V. Ivanova, A.R. Khamatgalimov, S.A. Katsyuba, Y.H. Budnikova, I.R. Nizameev, M.Yu. Balakina, J. Photochem. Photobiol. A 364 (2018) 764–772, https://doi.org/10.1016/j.jphotochem.2018.07.018.

[35] A.A. Kalinin, G.M. Fazleeva, T.I. Burganov, L.N. Islamova, Yu.B. Dudkina, A. A. Kadyrova, T.A. Vakhonina, A.R. Khamatgalimov, A.S. Mukhtarov, V.V. Bazarov, S.A. Katsyuba, Yu.H. Budnikova, M.Yu. Balakina, J. Photochem. Photobiol. A. 386 (2020), 112125, https://doi.org/10.1016/j.jphotochem.2019.112125.

[36] Y. H.Budnikova, Y. B.Dudkina, A. A.Kalinin, M. Yu.Balakina, Considerations on electrochemical behavior of NLO chromophores: relation of redox properties and NLO activity, Electrochim. Acta 368 (2021), 137578, https://doi.org/10.1016/j.electacta.2020.137578.

[37] A.A. Kalinin, L.N. Islamova, A.G. Shmelev, G.M. Fazleeva, O.D. Fominykh, Y. B. Dudkina, T.A. Vakhonina, A.I. Levitskaya, A.V. Sharipova, A.S. Mukhtarov, A. R. Khamatgalimov, I.R. Nizameev, Y.H. Budnikova, M.Y. Balakina, D-π-A chromophores with a quinoxaline core in the π-bridge and bulky aryl groups in the acceptor: synthesis, properties, and femtosecond nonlinear optical activity of the chromophore/PMMA guest-host materials, Dyes Pigment. 184 (2021) 108801, https://doi.org/10.1016/j.dyepig.2020.108801.

[38] G.M. Fazleeva, A.A. Kalinin, T.I. Burganov, L.N. Islamova, A.I. Levitskaya, T. A. Vakhonina, A.Sh. Mukhtarov, S.A. Katsyuba, M.Yu. Balakina, Synthesis and optical properties of chromophores with a methoxyphenylindolizine moiety, AIP Conf. Proc. 2390 (2022), https://doi.org/10.1063/5.0069249.

[39] A.A. Kalinin, M.A. Smirnov, L.N. Islamova, G.M. Fazleeva, T.A. Vakhonina, A. I. Levitskaya, O.D. Fominykh, N.V. Ivanova, A.R. Khamatgalimov, I.R. Nizameev, M.Yu. Balakina, Synthesis and characterization of new second-order NLO chromophores containing the isomeric indolizine moiety for electro-optical materials, Dyes Pigment. 147 (2017) 444–454, https://doi.org/10.1016/j.dyepig.2017.08.047.

[40] J.L. Oudar, D.S. Chemla, Hyperpolarisabilities of the nitroanilines and their relations to the excited state dipole moment, J. Chem. Phys. 66 (1977) 2664, https://doi.org/10.1063/1.434213.

[41] Y. Yang, F. Liu, H. Wang, J.Liu S.Bo, L. Qiu, Z. Zhen, X. Liu, Enhanced electro-optic activity from the triarylaminophenyl-based chromophores by introducing heteroatoms to the donor, J. Mater. Chem. C 3 (2015) 5297–5306, https://doi.org/10.1039/C5TC00723B.

[42] J.A. Davies, A. Elangovan, P.A. Sullivan, B.C. Olbricht, D.H. Bale, T.R. Ewy, et al., Rational enhancement of second-order nonlinearity:bis-(4-methoxyphenyl) heteroarylamino donor-based chromophores: design, synthesis, and electrooptic activity, J. Am. Chem. Soc. 130 (2008) 10565–10575, https://doi.org/10.1021/ja8007424.

[43] F. Liu, H. Wang, Y. Yang, H. Xu, D. Yang, S. Bo, J. Liu, Z. Zhen, X. Liu, L. Qiu, Using phenoxazine and phenothiazine as electron donors for second-order nonlinear optical chromophore: enhanced electro-optic activity, Dyes Pigment. 114 (2015) 196–203, https://doi.org/10.1016/j.dyepig.2014.11.015.

[44] N. Martínez de Baroja, J. Garín, J. Orduna, R. Andreu, M.J. Blesa, B. Villacampa, R. Alicante S. Franco, Synthesis, characterization, and optical properties of 4H-Pyran-4-ylidene donor-based chromophores: the relevance of the location of a thiophene ring in the spacer, J. Org. Chem. 77 (2012) 4634–4644, https://doi.org/10.1021/jo300373m.

[45] C. Rothe, D. Neusser, N. Hoppe, K. Dirnberger, W. Vogel, S. Gamez-Valenzuela, J. T. Lo pez Navarrete, B. Villacampa, M. Berroth, M.C. Ruiz Delgado, S. Ludwigs, Push–pull thiophene chromophores for electro-optic applications: from 1D linear to b-branched structures, Phys. Chem. Chem. Phys. 22 (2020) 2283–2294, https://doi.org/10.1039/c9cp05640h.

[46] M.J. Cho, J.Y. Kim, J.H. Kim, S.H. Lee, L.R. Dalton, D.H. Choi, Heterocyclic nonlinear optical chromophores composed of phenothiazine or carbazole donor and 2-cyanomethylene-3-cyano-4,5,5-trimethyl-2,5-dihydrofuran acceptor, Bull. Korean Chem. Soc. 26 (2005) 77–84, https://doi.org/10.5012/bkcs.2005.26.1.077.

[47] H. Zhang, Y. Yang, H. Xiao, F. Liu, F. Huo, L. Chen, Z. Chen, S. Bo, L. Qiu, Z. Zhen, Enhancement of electro-optic properties of bis(N,N-diethyl)aniline based second order nonlinear chromophores by introducing a stronger electron acceptor and modifying the π-bridge, J. Mater. Chem. C 5 (2017) 6704–6712, https://doi.org/10.1039/C7TC01175J.

[48] A.A. Kalinin, S.M. Sharipova, T.I. Burganov, A.I. Levitskaya, Y.B. Dudkina, A. R. Khamatgalimov, S.A. Katsyuba, Y.H. Budnikova, M. Yu. Balakina, High thermally stable D–π–A chromophores with quinoxaline moieties in the conjugated bridge: synthesis, DFT calculations and physical properties, Dyes Pigment. 156 (2018) 175–184.

[49] H. Zhang, H. Xiao, Z. Chen, F. Liu, F. Huo, S. Bo, L. Qiu, Z. Zhen, Improved electro-optical property by introducing stronger acceptor to thermal stable chromophores using modified julolidine as donor, Dyes Pigment. 167 (2019) 245–254, https://doi.org/10.1016/j.dyepig.2018.05.018.

[50] C. Hu, F. Liu, H. Zhang, F. Huo, Y. Yang, H. Wang, H. Xiao, Z. Chen, J. Liu, L. Qiu, Z. Zhen, X. Liu, S. Bo, Synthesis of novel nonlinear optical chromophores: achieving excellent electro-optic activity by introducing benzene derivative isolation groups into the bridge, J. Mater. Chem. C 3 (2015) 11595–11604, https://doi.org/10.1039/c5tc02702k.

[51] A.A. Kalinin, S.M. Sharipova, T.I. Burganov, Yu.B. Dudkina, A.R. Khamatgalimov, S.A. Katsyuba, Yu.H. Budnikova, M.Yu. Balakina, Push-pull isomeric chromophores with vinyl- and divinylquinoxalin-2-one units as π-electron bridge: synthesis, photophysical, thermal and electro-chemical properties, Dyes Pigment. 146 (2017) 82–91, https://doi.org/10.1016/j.dyepig.2017.06.062.

[52] T. Lu, F. Chen, Multiwfn: a multifunctional wavefunction analyzer, J. Comput. Chem. 33 (2012) 580–592, https://doi.org/10.1002/jcc.22885.

[53] R.Vijay Solomon, P. Veerapandian, S.A. Vedha, P. Venuvanalingam, Tuning nonlinear optical and optoelectronic properties of vinyl coupled triazene chromophores: a density functional theory and time-dependent density functional theory investigation, J. Phys. Chem. A 116 (2012) 4667–4677, https://doi.org/10.1021/jp302276w.

[54] H. Zhang, H. Huo, F. Liu, Z. Chen, J. Liu, S. Bo, Z. Zhen, L. Qiu, Synthesis and characterization of two novel second-order nonlinear optical chromophores based on julolidine donors with excellent electro-optic activity, RSC Adv 6 (2016) 99743–99751, https://doi.org/10.1039/c6ra21814h.

[55] H. Zhang, H. Xiao, F. Liu, F. Huo, Y. He, Z. Chen, X. Liu, S. Bo, L. Qiu, Z. Zhen, Synthesis of novel nonlinear optical chromophores: achieving enhanced electro-optic activity and thermal stability by introducing rigid steric hindrance groups into the julolidine donor, J. Mater. Chem. C 5 (2017) 1675–1684, https://doi.org/10.1039/c6tc05414e.